# RELATION BETWEEN $T_m$ AND DOMAIN SIZE OF CRYSTALLINE PHASE FOR PVIBE/ε-PL BLENDS AND ITS SAPONITE-CLAY NANOCOMPOSITES STUDIED BY SOLID-STATE NMR

Atsushi Asano[1*], Yoshifumi Murata[1], and Takuzo Kurotsu[1]

[1] Department of Applied Chemistry, National Defense Academy, Yokosuka, Japan

[*] Corresponding Author: asanoa@nda.ac.jp

**Abstracts: We studied the relationship between the domain size of crystalline phase (CR) of semicrystalline poly(ε-L-lysine) (ε-PL) and the melting points ($T_m$) of ε-PL in the poly(vinyl isobutyl ether) (PVIBE)/ε-PL blends and its saponite-clay nanocomposites. The domain size of CR is investigated by $^{13}$C cross-polarization with magic-angle-spinning nuclear magnetic resonance measurements. A two- or three-spin model was employed to obtain the $^1$H spin-diffusion rate between PVIBE and ε-PL by simulating the observed $^1$H spin-lattice relaxation curves. The thickness of lamellar layer in the CR phase is estimated by using both $^1$H spin-diffusion rate and degree of crystallinity. The obtained thickness of the CR phase is a total value as a sum of each CR domain but explains the shift of $T_m$ of ε-PL with increasing of PVIBE content reasonably.**

## Introduction

Microbial produced poly(ε-L-lysine) (ε-PL) is a water-soluble semicrystalline polymer and has attracted an attention as a novel biodegradable material, because it has property of safe for human beings and an antibacterial activity [1-3]. ε-PL is, however, too brittle and low degree of polymerization to use engineering purposes as it is. On the other hand, poly(vinyl isobutyl ether) (PVIBE) is a thermoplastic, elastic, and synthetic semicrystalline polymer. The physical and/or chemical properties of semicrystalline/semicrystalline polymer blends will be influenced by nanostructure, such as crystallinity, miscibility, domain size of crystalline phases. Therefore it is very important to characterize the nanostructure of semicrystalline polymer materials including natural rubber and elastomers.

In this study, we focused the relation between the melting point ($T_m$) and the domain size of crystalline phase for ε-PL in the blends of semicrystalline PVIBE and semicrystalline ε-PL. $T_m$ is known as to be obeyed by the Gibbs-Thomson relation; namely thicker layer of lamellar in a crystalline phase shows higher $T_m$. For a homogeneous blend, however, $T_m$ is governed by not only the thickness of lamellar but also the dilute effect of blending with PVIBE. By comparing the relation for the PVIBE/ε-PL blends and its saponite-clay nanocomposites, we concluded that lamellar thickness governs the shift of $T_m$ of ε-PL towards lower temperature with increasing of PVIBE. This study includes a part of results published in refs 4 to 6.

## Materials and Methods

ε-PL ([-NHCH$_2$CH$_2$CH$_2$CH$_2$CH(NH$_2$)CO-], relative molecular weight $M_w$ is 4,700, glass-transition temperature $T_g$ is 323 K, and $T_m$ is 445 K) was provided from Chisso Corporation as a solid powder. PVIBE ([-CH$_2$CH(OCH$_2$CH(CH$_3$)$_2$)-], $M_w$ = 600,000, $T_g$ = 253

K $T_m$ = 316 K) was obtained from Scientific Polymer Products, Inc. They were used without further purification. PVIBE and ε-PL were dissolved in chloroform/methanol mixed solvent, which the volume fraction is 9/1, at a concentration of 15 w/v%. The mixed ratios of PVIBE/ε-PL blends were 10/1, 10/2, 10/3, 10/4, and 10/5 by weight. The opaque and elastic films of the PVIBE/ε-PL blends were obtained from casting the respective chloroform/methanol=9/1 solutions on a Teflon plate at 313 K and further dried under vacuum at 313 K for 1 or 2 days. For the saponite clay nanocomposites, preparation was the same as that of the blends except for the mixing of saponite clay with ε-PL. To make the nanocomposites, the saponite-clay/ ε-PL mixed powder was used instead of ε-PL solid powder. The saponite-clay/ε-PL mixed powder was prepared by drying the ε-PL water dissolved with saponite-clay at 3 wt%. Saponite clay is a synthetic, a kind of smectite, and has a relatively small aspect ratio rather than that of montmorillonite clay. Furthermore, it has no paramagnetic center such as Fe$^{3+}$.

$^{13}$C NMR measurements were made using a Bruker DMX500 spectrometer operating at 125.76 MHz for $^{13}$C and 500.13 MHz for $^1$H. High-resolution solid-state $^{13}$C NMR spectra were obtained by the combined use of cross polarization (CP) and magic-angle spinning (MAS) with $^1$H high-power dipolar decoupling. $^{13}$C chemical shifts were measured relative to TMS using the methine carbon signal at 29.47 ppm for solid adamantane as an external standard. Details of how to measure the $^1$H and $^{13}$C spin-lattice relaxation times in the laboratory frame ($T_1^H$ and $T_1^C$), $^1$H spin-lattice relaxation times in the rotating frame ($T_{1\rho}^H$), and $^1$H spin-spin relaxation time ($T_2$) were described in refs 5 and 6.

The differential scanning calorimetry (DSC) was examined by using a Perkin-Elmer 7 system with increasing temperature at rate of 2 K·min$^{-1}$ from 233 K to 473 K.
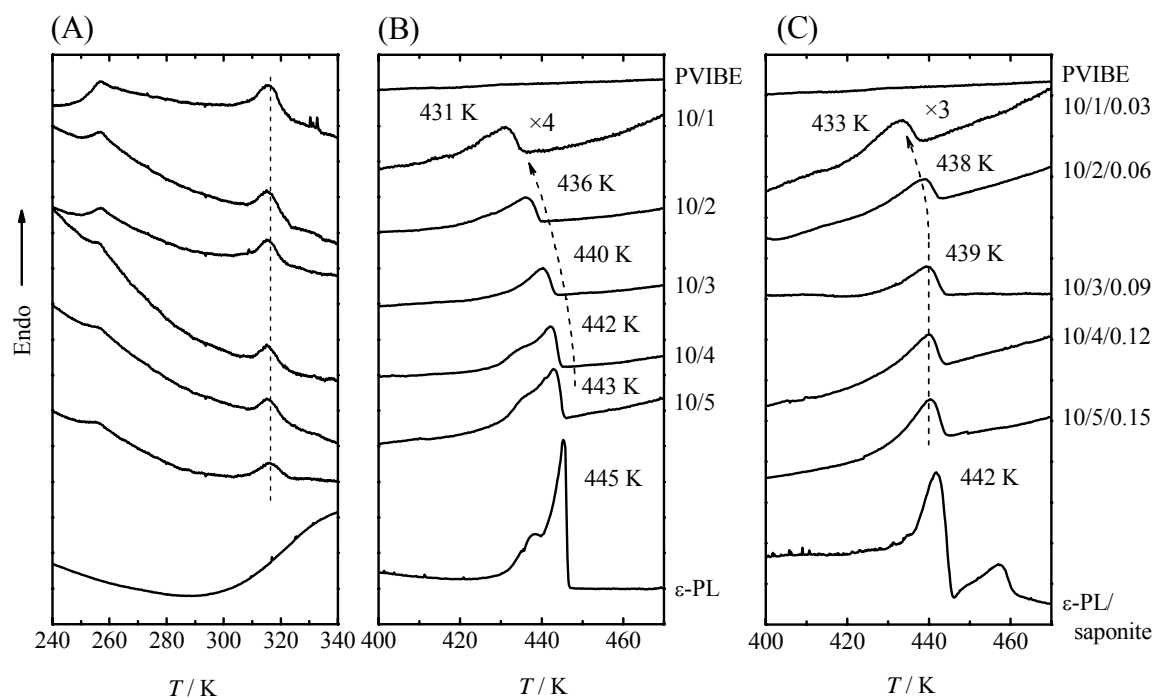
Figure 1. DSC curves for PVIBE (A, B, and C), PVIBE/ε-PL blends (A and B), PVIBE/ε-PL/saponite nanocomposites (C), and ε-PL (A, B, and C); A: thermal transitions of PVIBE. B and C: endothermic transition for melt of ε-PL.

## Results and Discussion

Figure 1 shows the observed and expanded DSC curves of pure PVIBE, PVIBE/ε-PL blends, nanocomposites, and pure ε-PL. Figure 1A represents mainly the thermal transition of PVIBE for pure PVIBE and PVIBE/ε-PL blends. Figure 1B and 1C show the melting point of ε-PL for PVIBE/ε-PL blends and PVIBE/ε-PL/saponite nanocomposites, respectively.

Every glass transition of PVIBE for PVIBE/ε-PL blends is observed at ca. 253 K, and every $T_m$ is detected at ca. 316 K (Figure 1A). Similarly, those thermal transitions of PVIBE in PVIBE/ε-PL/saponite nanocomposites were observed at the same point, too. These observations indicate that the blending of ε-PL or ε-PL/saponite does not affect the thermal transitions of PVIBE in both blends and nanocomposites.

However, it is apparently showed that the $T_m$ peak intensity of the crystalline phase of ε-PL decreases and shifts towards lower temperature from 445 to 431 K with increase of PVIBE content (Figure 1B and 1C). Furthermore, the values of $T_m$ of ε-PL in the PVIBE/ε-PL/saponite=10/3/0.09, 10/4/0.12, and 10/5/0.15 nanocomposites show the identical value of 439 K. This value is comparable to that of the PVIBE/ε-PL=10/3 blend (440 K).

The $T_m$ peak area, that is endothermic quantity, is related to the degree of crystallinity. Since we cannot obtain the 100 % complete crystal of ε-PL, the absolute value of crystallinity is not estimated easily. However, we can calculate the relative value for the blends and nanocomposites when the degree of crystallinity of ε-PL

is assumed to be approximately 60 %. The value of 60% was estimated and determined from comprehensive experiments of $T_1^C$, $^1H\ T_2$, and $^{13}C$ CPMAS NMR [4, 5]. The estimated values of crystallinity of ε-PL for the PVIBE/ε-PL=10/1 to 10/5 blends from DSC are 24, 58, 52, 61, and 62 %, respectively. Those values estimated from solid-state $^{13}C$ CPMAS NMR are 30, 58, 57, 55, and 59 %, respectively. Since both estimated values from DSC and NMR have an experimental error of about 5%, these values coincide with each other within an experimental error. This observation indicates that the growth of crystalline phase of ε-PL is not affected by blending with PVIBE, except for the PVIBE/ε-PL=10/1 blend.

The crystallinity of ε-PL for the PVIBE/ε-PL/saponite nanocomposites was similarly obtained from solid-state $^{13}C$ CPMAS NMR. The values were 36, 46, 47, 44, and 49 % from 10/1/0.03 to 10/5/0.15 compositions. These values are smaller than those of the PVIBE/ε-PL blends by about 10 %, except for the PVIBE/ε-PL/saponite=10/1/0.03 nanocomposite. The crystallinity of ε-PL/saponite was also decreased till 42% from 54%, which the value of 54 % is obtained from $^{13}C$ CPMAS NMR spectra for pure ε-PL. This observation shows that the mixing of saponite clay acts as an inhibitor for growing of lamellar layer in crystalline phase of ε-PL, in fact the $T_m$ of ε-PL after adding saponite clay decreases and becomes 442 K from 445 K (Figure 1C). Interestingly, furthermore, the crystallinity of PVIBE (about 20 %) in the nanocomposites was not affected by blending with ε-PL/saponite, although that in the blends decreases into the half (about 10%). This is probably caused by that
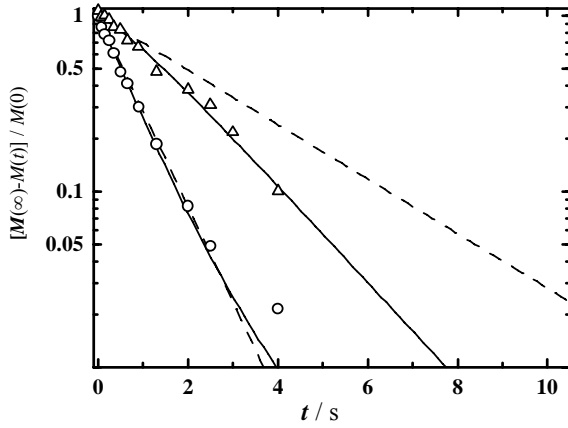
Figure 2. Observed $T_1^H$ relaxation curves of the PVIBE/ε-PL/saponite=10/2/0.06 nanocomposite. The symbols of circle are PVIBE and triangle ε-PL. Each solid line is calculated from equation (1). The broken lines represent the relaxation curves of pure PVIBE and pure ε-PL.

the small crystalline phase of ε-PL little affects the growth of crystalline phase of PVIBE. Because clay is hydrophilic but PVIBE is hydrophobic, saponite clay can not be close to PVIBE and will not affect the crystalline phase of PVIBE.

It is known that the shift of $T_m$ towards lower temperature relates the thickness of crystalline phase or diluent effect by adding PVIBE which $T_m$ is much lower than that of ε-PL. Figure 1A shows that the $T_m$ of PVIBE in the blends is not altered even at PVIBE/ε-PL=10/5, while the decrease of $T_m$ of ε-PL drastically occurs with increase of PVIBE. This indicates that PVIBE acts as a polymeric diluent for ε-PL, but ε-PL does not work as a diluent. If the diluent effect mainly governs the shift of $T_m$, the $T_m$ value of PVIBE will increase with the content of ε-PL. However, Figure 1A does not show the $T_m$ shift for PVIBE in the blends. Furthermore, the same $T_m$ value of ε-PL is observed for the PVIBE/ε-PL/saponite=10/3/0.09, 10/4/0.12, and 10/5/0.15 nanocomposites, even though the content of PVIBE is increased. Therefore, we can conclude that the shift of $T_m$ of ε-PL should be related on the thickness of lamellar layer in the crystalline phase.

To detect the domain size and thickness of lamellar layer of the crystalline phase, I examined the $^1$H spin-lattice relaxation curves observed from both PVIBE and ε-PL by taking into account the $^1$H spin-diffusion rate, which includes information of domain size. A CP from $^1$H to $^{13}$C enables us to detect the $^1$H decays for both PVIBE and ε-PL independently.

Figure 2 shows the observed $T_1^H$ relaxation curves for PVIBE (circle) and ε-PL (triangle) in the PVIBE/ε-PL/saponite=10/2/0.06 nanocomposite. The broken lines represent the $T_1^H$ relaxation curves for pure PVIBE and pure ε-PL, respectively. Since both polymers are semicrystalline polymer, we can observe both $T_1^H$ curves of the crystalline (CR) and the

non-crystalline (NC) phases for the respective polymer. For pure PVIBE and pure ε-PL, the observed $T_1^H$ curve of the CR phase showed the excellent agreement with that of the NC phase. Similarly, each $T_1^H$ curve of the CR phase for the PVIBE/ε-PL=10/2 to 10/5 blends and the corresponding nanocomposites was comparable to that of the NC phase. For the PVIBE/ε-PL=10/1 and PVIBE/ε-PL/saponite=10/1/0.03, however, the $T_1^H$ curve of CR of ε-PL did not coincide with that of NC, even though both relaxation curves for PVIBE agreed with each other.

The $T_1^H$ relaxation of ε-PL in Figure 2 decays faster than that of pure one. This indicates that $^1$H spin diffusion occurs efficiently between PVIBE and ε-PL in the PVIBE/ε-PL/saponite=10/2/0.06 nanocomposite. The $T_1^H$ relaxation of PVIBE, in contrast, does not change drastically. This phenomenon frequently appears when the spin has the relaxation rate faster than another spin in two- or three-spin system. Namely, slower relaxation curve is affected largely by $^1$H spin diffusion and becomes faster.

In order to analyze the observed $T_1^H$ curves, the two- or three-spin system for $^1$H spins was employed. By assuming $^1$H spin system as two-spin system, we can estimate the $^1$H spin-diffusion rate ($k$) between PVIBE and ε-PL domains. The $^1$H magnetization decay curves $M_A(t)$ and $M_B(t)$ for the A-B two-spin system can be given as follows: [7]

$$M_A(t) = a_+ e^{r_+ t} + a_- e^{r_- t}$$
$$M_B(t) = b_+ e^{r_+ t} + b_- e^{r_- t} \qquad (1).$$

Here, A and B denote PVIBE and ε-PL, respectively. Parameters $a_\pm$, $b_\pm$, and $r_\pm$ are expressed as follows:

$$a_\pm = \frac{1}{2}\left[1 \pm R^{-1} \cdot (K_B + k - K_A)\right], \quad r_\pm = \frac{1}{2}\left[-(K_A + K_B + k) \pm R\right],$$
$$b_\pm = \frac{1}{2}\left[1 \pm R^{-1} \cdot (K_A + k - K_B)\right],$$
$$R = \sqrt{\left[(K_A - K_B) + (f_B - f_A) \cdot k\right]^2 + 4 \cdot f_A \cdot f_B \cdot k^2}$$

Where $f_A$ and $f_B$ denote the $^1$H molar fractions of A and B spins, respectively. The initial magnetizations ratio $M_A(0):M_B(0)$ is assumed to be $f_A:f_B$. The calculated 'best-fit' curves are depicted as solid lines in Figure 2. The calculated curves are in good agreement with the observed data points. The obtained values are $K_A = 1.37$ s$^{-1}$, $K_B = 0.33$ s$^{-1}$, and $k = 0.38$ s$^{-1}$. The standard deviation is within 5 %.

When we assume that the domain is a lamellar structure [8], the repeating unit length ($L$; sum of each domain length of PVIBE and ε-PL) can be estimated to be 305 nm with both $^1$H spin-diffusion rate ($k$) and coefficient ($D$) of 380 nm$^2$s$^{-1}$, which is estimated by $^1$H spin-spin relaxation rate of the NC protons of PVIBE [9]. The $L$ is expressed by the following equation [8].

$$L = \frac{2\sqrt{D/\pi \cdot k}}{f_A \cdot f_B} \qquad (2).$$
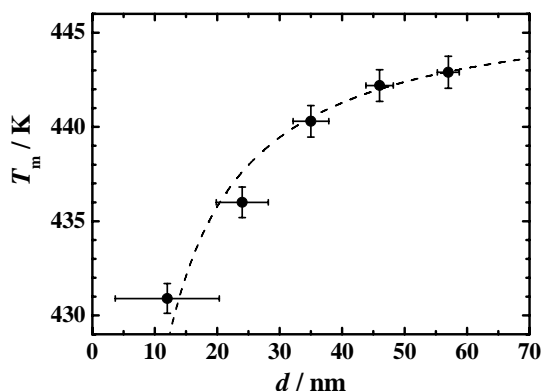
63

Figure 3. Plots of $T_m$ and the total CR thickness of ε-PL, $d$, for the PVIBE/ε-PL blends. The broken line is obtained from equation (3) by the least-square fit.

By multiplying the proton molar ratio of ε-PL in the PVIBE/ε-PL/saponite=10/2/0.06 nanocomposite to $L$ = 305 nm, we obtain the domain size of ε-PL to be 41 nm. Next, by multiplying the value of crystallinity (46 %) to 41 nm, we can estimate the total thickness of lamellar layers in the CR phase ($d$) to be 19 nm. Similarly, the $d$ values for the other blends and nanocomposites are obtained. For the PVIBE/ε-PL blends=10/1 to 10/5, the $d$ values were estimated to be 9.3, 29, 35, 46, 57 nm, respectively. For the PVIBE/ε-PL/saponite nanocomposites, the $d$ values were estimated to be 9.7, 19, 33, 30, 33 nm, respectively, from 10/1/0.03 to 10/5/0.15 compositions.

It is noteworthy that the total thickness of lamellar layer in the CR phase of ε-PL for the blends decreases gradually with the content of PVIBE. This change resembles in that of $T_m$ (Figure 1B). Furthermore, the constant $d$ value estimated for the PVIBE/ε-PL/saponite =10/3/0.09, 10/4/0.12, and 10/5/0.15 coincides with the change of $T_m$ (Figure 1C). Moreover, this $d$ value of 30-33 nm is comparable to that obtained from the PVIBE/ε-PL=10/3 blend (35 nm), as it is expected from $T_m$ value. These results strongly suggest that the shift of $T_m$ toward lower temperature with increasing of PVIBE is related to the thickness of crystalline phase.

According to the Gibbs-Thomson effect, the depression of $T_m$ is inversely proportional to the CR thickness as following equation [10].

$$T_m(x) = T_m{}^0 - \frac{\theta}{x}, \quad \theta = 2\sigma \cdot T_m{}^0 / \Delta H_m{}^0 \quad (3).$$

Here, $T_m{}^0$, σ, $\Delta H_m{}^0$, and $x$ are, respectively, $T_m$ of a complete crystal of ε-PL, surface energy at the lamella interface, equilibrium enthalpy per a unit cell, and the thickness of a lamellar. The broken line in Figure 3 is the least-square fitted curve to the data points by substituting $x$ to $d$. The fitted curve is in excellent agreement with the observed data points. The estimated $T_m{}^0$ and θ are 446.8 ± 0.2 K and 220 ± 10 K·nm, respectively. The value of $T_m{}^0$ is a little larger than that

obtained $T_m$ from pure ε-PL. This is reasonable because pure ε-PL does not form a complete crystal.

These $T_m{}^0$ and θ values give the σ / $\Delta H_m{}^0$ of ca. 0.25. When the $\Delta H_m{}^0$ value is assumed to be calculated from DSC measurement of pure ε-PL (assuming 60% crystallinity), we can obtain the surface energy at the lamella interface σ of ca. 3.5 kJ·mol$^{-1}$ ($\Delta H_m{}^0$ = ca. 14 kJ·mol$^{-1}$). Unfortunately, we could not know the σ values for almost all semicrystalline polymers, so that we can not discuss whether the estimated value is correct or not. However, for general semicrystalline polymers, the value of $T_m{}^0$ / $\Delta H_m{}^0$ becomes 10 to 100 K·mol·kJ$^{-1}$ [11], especially, the value of nylon 6 is 21 K·mol·kJ$^{-1}$. In the ε-PL case, which has a resemble unit structure to nylon 6, the value becomes 32 K·mol·kJ$^{-1}$. Therefore, the surface energy at the lamella interface estimated here is satisfactorily reliable.

## Conclusions

We showed that $T_m$ of ε-PL in PVIBE/ε-PL blends gradually shifts toward lower temperature with increase of PVIBE component. Similarly, for PVIBE/ε-PL/ saponite nanocomposites, $T_m$ of ε-PL shifts to lower temperature by adding saponite clay and shows large shift at large PVIBE compositions. Furthermore, $T_m$ is constant for PVIBE/ε-PL/saponite=10/3/0.09 to 10/4/0.15, even though $T_m$ of ε-PL in the blends alters. From solid-state $^{13}$C CPMAS NMR analyses, it is revealed that the change of $T_m$ of ε-PL comes from the change of thickness of lamellar layers in the crystalline phase of ε-PL.

## References

1. SHIH, I.-L. SHEN, M.-H. AND VAN, Y.-T., *Bioresource Technology*, **97**, p.1148-1159 (2006).
2. MAEDA, S. KUNIMOTO, K. SASAKI, C. KUWAE, A. AND HANAI, K., *J. Mol. Struc.*, **655**, 149-155 (2003).
3. MAEDA, S. MORI, T. SASAKI, C. KUNIMOTO, K. KUWAE, A. AND HANAI, K., *Polym. Bull.*, **53**, 259-267 (2005).
4. ASANO, A. MURATA, Y. AND KUROTSU T., IRC2005 Conf. Proc., Yokohama, Japan, 2005, (P-05) p.1-8.
5. ASANO, A. MURATA, Y. AND KUROTSU T., *e-Journal Soft Mater.*, **3**, 1-8 (2007).
6. ASANO, A. TANAKA, C. AND MURATA, Y., *Polymer*, **48**, 3809-3816 (2007).
7. STEJSKAL, E.O. SCHAEFER, J. SEFCIK, M.D. MCKAY, R.A., *Macromolecules*, **14**, 275-279 (1981).
8. VANDERHART, D.L. AND MCFADDEN, G.B., *Solid State Nuc. Magn. Reson.*, **7**, 45-66 (1996).
9. ASSINK, R. A. *Macromolecues*, **11**, 1233-1237 (1978).
10. STROBL, G.R., *The Physics of Polymers*, 2$^{nd}$ ed. (Springer-Verlag, Berlin, Heidelberg, 1997) Chapter 4.
11. WUNDERLICH, B., *Thermmal Analysis*, (Academic Press, 1990).